Received: 5 October 2018 | Revised: 8 February 2019 | Accepted: 11 February 2019

DOI: 10.1002/glia.23606

GLIA

WILEY

RESEARCH ARTICLE

Inhibition of MAPK/ERK pathway promotes oligodendrocytes generation and recovery of demyelinating diseases

Na Suo[1,2] | Yu-e Guo[1,2] | Bingqing He[1,2,3] | Haifeng Gu[1] | Xin Xie[1,3,4]

[1]CAS Key Laboratory of Receptor Research, the National Center for Drug Screening, Shanghai Institute of Materia Medica, Chinese Academy of Sciences, Shanghai, China

[2]University of Chinese Academy of Sciences, Graduate School, Beijing, China

[3]School of Life Science and Technology, ShanghaiTech University, Shanghai, China

[4]Stake Key Laboratory of Drug Research, Shanghai Institute of Materia Medica, Chinese Academy of Sciences, Shanghai, China

Correspondence
Xin Xie, CAS Key Laboratory of Receptor Research, the National Center for Drug Screening, Shanghai Institute of Materia Medica, Chinese Academy of Sciences, 189 Guo Shou Jing Road, Shanghai 201203, China.
Email: xxie@simm.ac.cn

Funding information
Ministry of Science and Technology of China, Grant/Award Numbers: 2015CB964503, 2017YFA0104002; Chinese Academy of Sciences, Grant/Award Number: XDA16010202; National Natural Science Foundation of China, Grant/Award Numbers: 81425024, 81730099, 81472862

Abstract

Oligodendrocytes (OLs) are the myelinating glia of the central nervous system. Injury to OLs causes myelin loss. In demyelinating diseases, such as multiple sclerosis, the remyelination is hindered principally due to a failure of the oligodendrocyte precursor cells (OPCs) to differentiate into mature OLs. To identify inducers of OPC to OL differentiation, a high-throughput screening based on myelin basic protein expression using neural progenitor cells-derived OPCs has been performed and, PD0325901—an MEK (MAPK kinase) inhibitor—is found to significantly enhance OPC to OL differentiation in a dose- and time-dependent manner. Other MEK inhibitors also display similar effect, indicating blockade of MAPK–ERK signaling is sufficient to induce OPC differentiation into OLs. PD0325901 facilitates the formation of myelin sheaths in OPC–neuron co-culture in vitro. And in experimental autoimmune encephalomyelitis model and cuprizone-induced demyelination model, PD0325901 displays significant therapeutic effect by promoting myelin regeneration. Our results suggest that targeting the MAPK–ERK pathway might be an intriguing way to develop new therapies for demyelinating diseases.

KEYWORDS

differentiation, ERK, MAPK, MEK inhibitor, myelin, oligodendrocyte, oligodendrocyte progenitor cell, remyelination

1 | INTRODUCTION

Myelin is a unique structure of the nervous system and is often considered as the electrical insulator on nerve fibers. As a matter of fact, myelin sheath not only enables rapid impulse conduction but also plays fundamental roles in modulating information flow within neural circuits and providing metabolic support for axons (Funfschilling et al., 2012; Lappe-Siefke et al., 2003; Morrison, Lee, & Rothstein, 2013; Nave & Werner, 2014; Saab, Tzvetanova, & Nave, 2013). In the central nervous system (CNS), the myelinating cells are known as oligodendrocytes (OLs), a specialized type of glial cells originating from the neural stem cells (Bergles & Richardson, 2015; Takebayashi & Ikenaka, 2015).

Developmentally, oligodendrocyte precursor cells (OPCs) give rise to immature (or premyelinating) and then mature (or myelinating) OLs that wrap neuronal axons and form myelin sheath (Emery, 2010; van Tilborg et al., 2018). OPCs specifically express platelet-derived growth factor receptor (α-subunit, PDGFRα) and chondroitin sulfate proteoglycan neuron-glia antigen 2 (NG2) (Bergles & Richardson, 2015; Goldman & Kuypers, 2015), which are downregulated when OPCs go into differentiation. During the differentiation process, O4, O1, 2′,3′-cyclic nucleotide-3′-phosphohydrolase (CNPase), myelin basic protein (MBP), proteolipid protein (PLP), and myelin oligodendrocyte glycoprotein (MOG) are gradually expressed in an orderly manner (Barateiro & Fernandes, 2014; Craig et al., 2003; Scolding et al., 1989; Zhang, 2001).

Injury to OLs causes myelin loss, also termed demyelination. After acute demyelination, OPCs, as widely distributed and abundant in adult CNS, migrate to the lesion and differentiate into mature OLs which remyelinate the axons (Franklin, 2002; Franklin & Ffrench-Constant, 2008; Gensert & Goldman, 1997). In demyelinating diseases such as multiple sclerosis, remyelination by adult OPCs is hindered principally due to

a failure of OPCs to differentiate into mature OLs (Chang, Nishiyama, Peterson, Prineas, & Trapp, 2000; Keirstead, Levine, & Blakemore, 1998; Woodruff, Fruttiger, Richardson, & Franklin, 2004). Therefore, identification of pathways and small molecules that promote OPC differentiation, remyelination, and functional recovery has received much attention. Through image-based screen, benztropine has been identified to enhance remyelination by direct antagonism of M1 and/or M3 muscarinic receptors (Deshmukh et al., 2013). Mei et al. (2016) carried out a screen focusing on GPCR modulators and identified 12 kappa-opioid receptor (KOR) agonists that enhance OPC to OL differentiation. Their study is consistent with Du et al.'s finding that U50488 targeting KOR ameliorates symptoms of EAE by promoting remyelination rather than immune suppression (Du et al., 2016). Another screen of NIH Clinical Collection I and II libraries has also identified two drugs—miconazole and clobetasol—which are effective in promoting OL generation in vitro and remyelination in vivo (Najm et al., 2015). We also developed a high-throughput screening assay based on the induction of MBP during OPC to OL differentiation, and vitamin C has been found to greatly promote OL differentiation, maturation, and remyelination (Guo, Suo, Cui, Yuan, & Xie, 2018).

Here we report the discovery that small molecule inhibitors of MAPK/ERK pathway, represented by PD0325901, significantly promote OPC to OL differentiation and myelin formation. In immune- and drug-mediated demyelination animal models, PD0325901 also shows significant therapeutic effects.

2 | MATERIALS AND METHODS

2.1 | Reagents

Laminin, poly-ornithine, thyroid hormone (T3), paraformaldehyde (PFA), bis(cyclohexanone)oxaldihydrazone (Cuprizone), Hoechst 33342, poly-D-lysine, papain, L-cysteine, insulin, transferrin, progesterone, putrescine, BSA, and 5-fluoro-2′-deoxyuridine were purchased from Sigma-Aldrich. Collagenase A was purchased from Roche. EGF, bFGF, and PDGF-AA were purchased from Peprotech. PD0325901, CI-1040, AZD8330, and AZD6244 were purchased from MedChemExpress, and U0126 was purchased from Tocris.

2.2 | OPC differentiation

Neural progenitor cells (NPCs) were purified from the dissected cerebral cortex of E14.5 mouse embryos by suspension culture (Chen et al., 2007). NPCs were expanded as neurospheres in the NPC medium (DMEM/F12 (Gibco) supplemented with 20 ng/ml EGF, 20 ng/ml bFGF, 2% B27 (Invitrogen), 100 units/ml penicillin, and 100 μg/ml streptomycin). Neurospheres were passaged every 2 days and never allowed to reach confluence. Neurospheres from Passages 3–5 were used for the differentiation assay. To generate OPCs, neurospheres were dissociated into single cells with accutase (Millipore, SF006) and seeded onto poly-ornithine (5 μg/ml) plus laminin (1 μg/ml)-coated plates in OPC medium (DMEM/F12 supplemented with 10 ng/ml bFGF, 10 ng/ml PDGF-AA, 2% B27, 100 units/ml penicillin, and 100 μg/ml streptomycin). Two days later, PDGF-AA and bFGF were withdrawn to induce OPC differentiation (OL medium), and cells were stimulated with compounds or DMSO control for another 4–5 days.

2.3 | High-throughput screening and imaging

For the primary screen, neurospheres were dissociated into single cells and seeded at a density of 8,000 cells per well onto poly-ornithine (5 μg/ml) plus laminin (1 μg/ml)-coated 96-well plates in OPC medium for 2 days. Then OPCs were induced to differentiation into OLs as previously described. And various compounds at a concentration of 20 μM were added at the same time. Thyroid hormone T3 (100 nM) and DMSO (0.2%, v/v) were included in each assay plate as positive and vehicle controls. Four days later, cells were fixed with 4% paraformaldehyde (PFA) and stained with mouse anti-rat MBP antibody (Covance, SMI-94R, 1:500) and secondary antibody conjugated to Alexa Fluor 488 (Thermo Fisher, A-11001, 1:1,000). Hoechst 33342 was used to identify cell nuclei. Eleven images per well (representing different locations in a single well) were captured and the nuclei and MBP-positive cells were quantified using the Operetta high content analysis system (PerkinElmer).

2.4 | Immunofluorescence staining

Cells were fixed with 4% PFA in phosphate-buffered saline (PBS) for 15 min at room temperature and blocked in PBS containing 1% BSA and 0.3% Triton for 30 min at room temperature. Then cells were incubated with the relevant primary antibody at 4°C overnight and the appropriate fluorescence-conjugated secondary antibody for 1 hr at room temperature. Nuclei were stained with Hoechst 33,342 (10 mg/ml). Antibodies used in this assay were as follows: anti-MBP (Covance, SMI-94R, 1:500), anti-NF-200 (Sigma, N4142, 1:1000), anti-O4 (R&D Systems, MAB1326, 1:1200), and anti-CNPase (Millipore, MAB326, 1:1200).

2.5 | OPC–DRG neuron co-culture

Dorsal root ganglions (DRGs) isolated from P5-P10 C57BL/6 pups were incubated in Hank's balanced salt solution (HBSS) containing papain (3 U/ml) and L-cysteine (0.36 mg/ml) for 10 min at 37°C. After removal of papain solution, DRGs were further incubated in HBSS containing collagenase A (100 U/ml) for 10 min at 37°C. After thorough washing, the dissociated DRG neurons were seeded at a density of 20,000 cells/well onto poly-D-lysine (80 μg/ml) and rat tail collagen (25 μg/ml) coated 48-well plate and maintained in myelination medium (DMEM (Gibco), 2% B27, 1% Glutamax (Gibco), insulin (5 μg/ml), transferrin (50 μg/ml), 0.5% FBS, progesterone (0.2 μM), putrescine (100 μM), BSA (0.1 mg/ml), sodium selenite (5 ng/ml), 100 units/ml penicillin, and 100 μg/ml streptomycin) for 9 days, and 5-fluoro-2′-deoxyuridine (10 μM) was added to remove contaminating glia cells for the first 7 days. After 9 days, 3×10^4 OPCs freshly isolated from P0–P2 C57BL/6 pups cortices with anti-AN2 microbeads (Miltenyi) were added per well to DRG neurons, and the co-cultures were maintained for another 6 days in myelination medium. Drugs were added after the addition of OPCs. Cultures were fixed and stained with anti-NFH (Sigma) and anti-MBP (Covance) antibodies. Images (47 pictures/well)

were taken and analyzed using the Operetta high content analysis system, and myelination was identified as neuritis double positive for MBP and NFH staining.

2.6 | EAE model

C57BL/6 mice (8–10 weeks) were immunized subcutaneously with 200 μg MOG_{35-55} (MOG, GL BioChem [Shanghai], 051716) emulsified in CFA (CFA, Sigma, F5506), which contains 0.5 mg *Mycobacterium tuberculosis* (MT, BD, BD-231141) followed by intraperitoneal injection with *Bordetella pertussis* toxin (PTX, 200 ng per mouse, Millipore, 516561) on Days 0 and 2. For drug treatment, the mice receive daily intraperitoneal injection of PD (5 mg/kg) buffered in PBS with 1% DMSO or vehicle control (PBS with 1% DMSO) from Day 3 postimmunization. The disease severity was scored daily.

2.7 | Cuprizone-induced demyelination mouse model

Female C57BL/6 mice (9 weeks) were fed with 0.2% (w/w) cuprizone (Bisoxaldihydrazone, Sigma, C9012) mixed into a ground standard rodent chow. Cuprizone diet was maintained for 5 weeks; thereafter cuprizone-infused food was removed and the animals were given a standard normal chow. PD was dissolved in saline with 1% DMSO and daily i.p. injections were initiated at the withdrawal of the cuprizone diet. At different time points (0, 1, and 2 weeks after cuprizone withdrawal), animals were anesthetized and perfused with PBS followed by 4% PFA. Brains were removed and fixed in 4% PFA overnight, and then sectioned and stained for histopathological analysis. All the mice were maintained in pathogen-free conditions, and all experimental procedures were approved and conducted in accordance with international guidelines for the care and use of laboratory animals and were approved by the Animal Ethics Committee of Shanghai Institute of Materia Medica.

2.8 | Histology and immunohistochemical analysis

Paraffin-embedded coronal sections of brains were stained with Luxol fast blue (LFB, Sigma, S3382) to assess remyelination. Images were taken and quantitative image analysis was performed using Image-Pro Plus. Region of corpus callosum was initially marked using the "irregular AOI" tool, blue areas were then counted within the lesion using the "count and measure objects" tool. Percentage of the remyelination area was calculated by the ratio of the blue area and total corpus callosum area. For immunofluorescent analysis, frozen sections of brains and spinal cords were blocked and permeated with PBS containing 2.5% BSA and 0.3% Triton-X 100 for 45 min at room temperature, then incubated with mouse anti-MBP antibody (Covance, SMI-94R, 1:500), mouse polyclonal anti-MOG antibody (Millipore, AB5320, 1:500) and rabbit polyclonal anti-GST-pi antibody (Millipore, AB5320, 1:500), rabbit anti-PDGFRα (Cell signaling, 3164S, 1:200), and rabbit anti-NG2 (Millipore, AB5320, 1:200) at 4°C overnight. After thorough washing, the sections were stained with secondary antibody conjugated to Alexa Fluor 488 or Alexa Fluor 555 (Thermo Fisher, 1:1,000) for 1 hr at room temperature, and nuclei were stained with Hoechst 33342. Images were taken using an Olympus IX71 inverted fluorescent microscope, and quantitative image analysis was performed using Image-Pro Plus.

2.9 | Electron microscopy

Spinal cords and brains were isolated from 4% PFA perfused mice, and fixed in 4% PFA overnight. Demyelinated white matter of the spinal cords and corpus callosum of the brains were isolated and fixed in PBS buffered 2.5% glutaraldehyde for 2 hr at room temperature. Then the samples were washed, fixed in 1% osmium tetroxide, subsequently dehydrated in graded acetone series, and embedded in EPON. Thin sections of 70 nm were cut with a diamond knife and mounted on copper slot grids coated with Formvar and stained with uranyl acetate and lead citrate for examination on JEM-1230 transmission electron microscope. *G*-ratios were measured in Image-Pro, and ∼200 remyelinated axons were measured for each group.

2.10 | Reverse transcription and PCR

Total RNA was extracted with Trizol (Invitrogen). One microgram of RNA was used to synthesize cDNA using the PrimeScript RT Reagent Kit (Takara Bio, RR037A) according to the manufacturer's protocol. Real-time PCR was performed using the FastStart Universal Probe Master Mix (Bimake, B21702) and a Stratagene Mx3000P thermal cycler. Primer sequences are as follows: MBP, sense (5′-TGACACCTC-GAACACCACCTC-3′) and antisense (5′-CCTTGAATCCCTT- GTGAGCC -3′); MAG, sense (5′-GGTGTTGAGGGAGGCAGTTG-3′) and antisense (5′-CGTTCTCTGCTAGGCAAGCA-3′); MOG, sense (5′-AGCTGCTTCC TCTC- CCTTCTC-3′) and antisense (5′-ACTAAAGCCCGGATGGGATAC -3′); CNP, sense (5′-TCCACGAGTGCAAGACGCTATTCA-3′) and antisense (5′-TGTAAGCATC- AGCGGACACCATCT-3′); PLP, sense (5′-TGC TCGGCTGTACCTGTGTACAT- T-3′) and antisense (5′-TACATTCTGG CATCAGCGCAGAGA-3′); GAPDH, sense (5′-AGGTCGGTGTGAACGG ATTTG-3′) and antisense (5′-TGTAGACCATGT- AGTTGAGGTCA-3′).

2.11 | Western blot

OLs differentiated from NPC-derived OPCs were lysed and boiled at 95–100°C for 10 min in sample buffer (50 mM Tris–HCl, 2% w/v SDS, 10% glycerol, 1% β-mercaptoethanol, 0.01% bromophenyl blue [pH 6.8]). Total proteins of each sample were separated on 10%–15% SDS-PAGE gels and transferred onto PVDF (polyvinylidene difluoride, Millipore) membranes. The membranes were first incubated with blocking buffer (TBS with 0.1% Tween 20, 10% nonfat milk) for 1 h at room temperature and then incubated with rabbit anti-GAPDH (CST, 2118, 1:8000), rabbit anti-ERK (CST, 9102, 1:1000), rabbit anti-p-ERK (CST, 4370, 1:1000), and rat anti-MBP (Covance, SMI-94R, 1:1000) overnight at 4°C. After thorough washing, the membranes were incubated with anti-rabbit IgG HRP (CST, 1:8000) or anti-rat IgG HRP (CST, 1:8000) for 1 hr at room temperature. After through washing, blots were visualized using Amersham ECL Plus Western Blotting detection reagents (GE Healthcare).

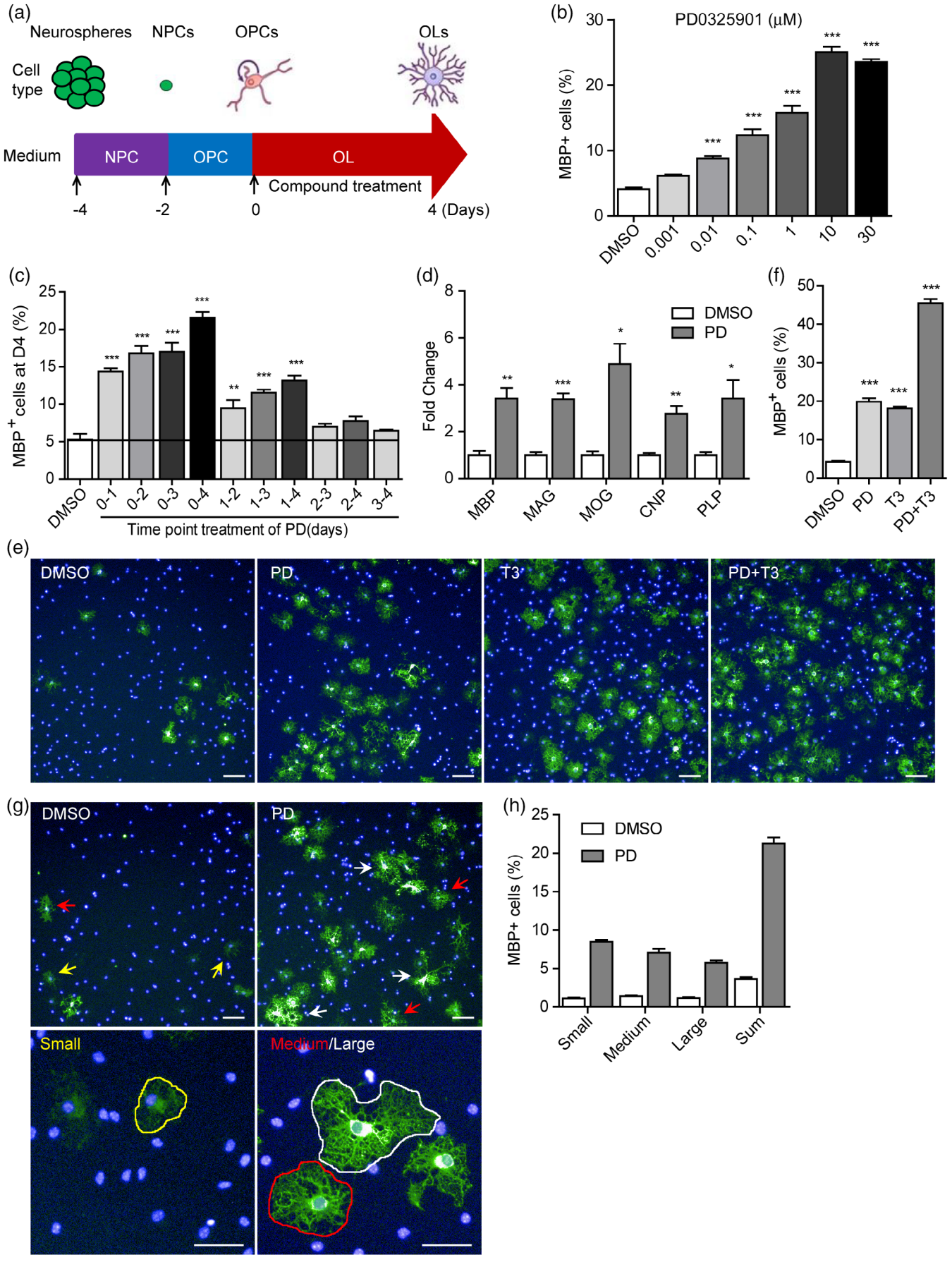

FIGURE 1 Legend on next page.

2.12 | Statistical analysis

Data were analyzed with GraphPad Prism software. For comparison between two groups, statistical evaluation was done by two-tailed Student's *t* test. Two-way analysis of variance test was used to assess the significance between treatment groups of EAE animals. For multiple comparisons, one-way ANOVA test was used. For all statistical tests, the *p* values <.05 were considered statistically significant. All error bars show standard error of the mean (SEM).

3 | RESULTS

3.1 | PD0325901 promotes the generation of MBP$^+$ cells from NPC-derived OPC in vitro

To identify drug-like small molecules that can induce OPC differentiation, we developed a high-content imaging assay based on MBP expression (Guo et al., 2018). Briefly, cortical NPCs from mouse E14.5 embryos were expended in vitro as neurospheres. NPCs were then differentiated into OPCs with typical bipolar or tripolar morphology. Then the OPCs were further differentiated into MBP$^+$ mature OLs by culturing in OL medium for 4 days. Various compounds at 20 μM were added during OPC to OL differentiation (Day 0, Figure 1a), and the percent of MBP$^+$ cells at Day 4 were used as readout. Seven thousand three hundred and forty-seven compounds from the Chinese National Compound Library were screened and a number of compounds, including vitamin C, were found to enhance the generation of MBP$^+$ cells (Guo et al., 2018).

Among these compounds, an MEK inhibitor, PD0325901, was found to dose-dependently increase the percentage of MBP$^+$ cells ($EC_{50} \sim 100$ nM) (Figure 1b). We decided to investigate this compound further because it is an orally available compound that readily crosses the blood–brain barrier (Lopez-Juarez et al., 2017). The time-dependent effect of PD0325901 was also studied by adding 10 μM of the compound into the OL medium for various durations (Figure 1c). The results indicate that the early addition of PD0325901 was important. Treatment with PD0325901 for only one day at the starting stage resulted in significant increase in MBP$^+$ cells (Figure 1c). In contrast, PD0325901 treatment after Day 2 had very limited effect (Figure 1c). QPCR analysis also demonstrated that a number of OL markers, including MBP, myelin associated glycoprotein (MAG), myelin oligodendroglial glycoprotein (MOG), 2′,3′-cyclic nucleotide 3′-phosphodiesterase (CNPase), and PLP, were significantly increased in PD0325901-treated group (Figure 1d). In PD0325901 (10 μM)-treated OPCs, more than 20% of the cells became MBP$^+$ at Day 4 (Figure 1e,f). The induction efficiency was even slightly higher than the known OL inducer T3 (500 nM) (Figure 1e,f). More interestingly, PD0325901 and T3 showed an additive effect in inducing MBP$^+$ cells, suggesting that these two compounds might act through different mechanisms (Figure 1e,f).

Mature OLs typically possess complicated membrane processes and are larger in size than the immature OLs. We carefully categorized the MBP$^+$-OLs into three groups by cell area: small (600–2,000 μm^2, yellow arrow and circle), medium (2,000–4,000 μm^2, red arrow and circle) and large (>4,000 μm^2, white arrow and circle) size OLs (Figure 1g). PD0325901 enhanced the generation of small, medium, and large size OLs to a similar extent (Figure 1h).

To further confirm the effect of PD0325901 on OL generation, gradual expression of multiple markers representing various differentiation stages of OLs were studied. At early stage of differentiation, OPCs give rise to pre-OLs that express O4 (Barateiro & Fernandes, 2014; Zhang, 2001). PD0325901 treatment significantly increased O4$^+$ cell numbers from Day 1 (Figure 2a,b). CNPase, expressed slightly later than O4 during OL maturation (Barateiro & Fernandes, 2014; Zhang, 2001), could be detected as early as day 2 in PD0325901-treated cells (Figure 2c,d). While in DMSO-treated cells, the expression of CNPase was delayed for at least one day and CNPase$^+$ cells with clear membrane processes could only be observed after Day 4 (Figure 2c,d). And the expression of MBP, a marker of mature OLs, could be detected from Day 3 in PD0325901-treated cells, one day earlier than the DMSO control. The percentages of O4$^+$MBP$^+$ OLs were also significantly higher in PD0325901-treated cells compared with DMSO control at all three time points analyzed (Figure 2a, e). Combining the data from Figure 1c, these results indicate that PD0325901 exerts its effect at early stage of OL differentiation. PD0325901 promotes the OPC to OL fate determination, and once more immature OLs are generated, more mature OLs will be obtained.

3.2 | Inhibition of ERK/MAPK pathway promotes OL generation

PD0325901 is a well-known second generation analog of CI-1040, the first MEK (an MAPK kinase) inhibitor to enter clinical evaluation (Sebolt-Leopold et al., 2004). Therefore, a panel of reported MEK inhibitors, including AZD8330, AZD6244, U0126, and CI-1040 (Akinleye,

FIGURE 1 PD0325901 promotes OPC to OL differentiation. (a) Procedures of OL differentiation from neurospheres generated from cortical NPCs of mouse E14.5 embryos: neurosphere formation (NPC medium), OPC differentiation (OPC medium), and OL differentiation and maturation (OL medium). (b) Dose-dependent effect of PD0325901 in inducing OPC differentiation into mature OLs. OPCs were treated with PD0325901 for 4 days. ***p < .001 (one-way ANOVA followed by Dunnett's multiple comparison test). (c) Time-dependent effect of PD0325901 (10 μM) in inducing OPC to OL differentiation. **p < .01, ***p < .001 (one-way ANOVA followed by Dunnett's multiple comparison test). (d) Real-time q-PCR analysis of myelin-associated genes in OLs differentiated from NPC-derived OPCs in the presence of PD0325901 (10 μM) or not for 4 days. Results were normalized to GAPDH in the same sample and then normalized to the DMSO group. *p < .05, **p < .01, ***p < .001 (Student's *t* test). (e) Mouse NPC-derived OPCs were differentiated in the presence of PD0325901 (10 μM), T3 (500 nM), or the combination of both for 4 days. OLs were stained with antibody against MBP (green). Nuclei were stained with Hoechst (blue). Scale bars, 100 μm. (f) Statistical analysis of the MBP$^+$ cells in (e). Data are representative of three independent experiments, means ± SEM (n = 4). ***p < .001 (one-way ANOVA followed by Dunnett's multiple comparison test). (g) Typical morphology of large (>4,000 μm^2, white arrow and circle), medium (2,000–4,000 μm^2, red arrow and circle), and small (600–2,000 μm^2, yellow arrow and circle) size OLs. Cells were stained with antibody against MBP (green). Nuclei were stained with Hoechst (blue). Scale bars, top panels, 100 μm; bottom panels, 50 μm. (h) Statistical analysis of the MBP$^+$ cells in (g) [Color figure can be viewed at wileyonlinelibrary.com]

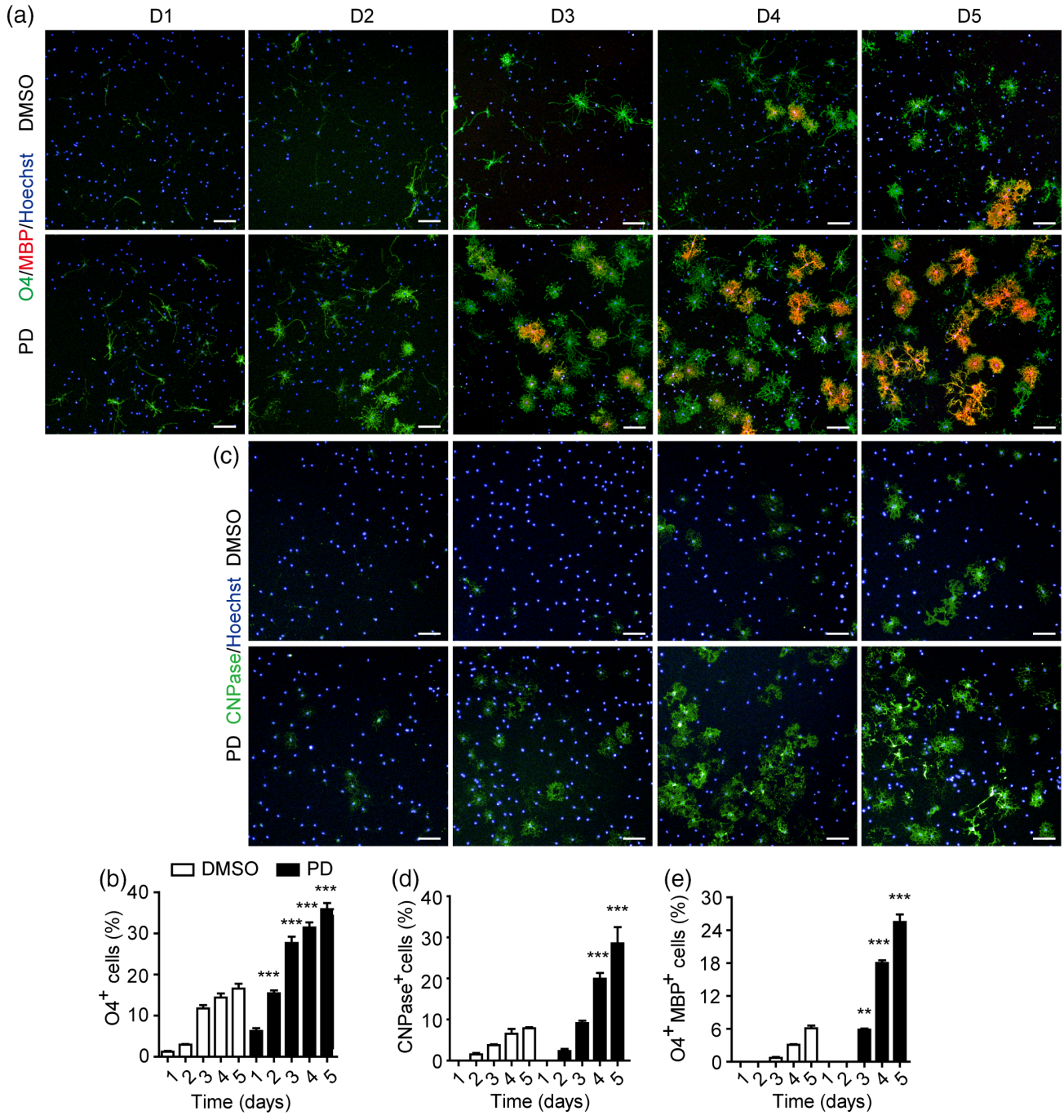

FIGURE 2 PD0325901 promotes gradual expression of OL lineage markers. (a,c) NPC-derived OPCs were differentiated in the presence of PD (10 μM) or vehicle (DMSO) for 1–5 days. The expression of O4 (a), CNPase (c), and MBP (a) were detected by immunofluorescence staining. Scale bars, 100 μm. (b,d,e) Statistical analysis of $O4^+$ (b), $CNPase^+$ (d), and $O4^+MBP^+$ (e) cells in (a,c). Data are means ± SEM ($n = 3$), $^{**}p < .01$, $^{***}p < .001$ versus DMSO control at the same date (one-way ANOVA followed by Tukey's multiple comparison test) [Color figure can be viewed at wileyonlinelibrary.com]

Furqan, Mukhi, Ravella, & Liu, 2013; Planz, 2013), were also evaluated in OPC to OL differentiation assay. As demonstrated in Figure 3a,b, all inhibitors could induce OPC to OL differentiation in a dose-dependent manner with various efficacies. The best effect of AZD8330 was comparable to PD0325901, ~25% of the cells became MBP^+ when treated with these compounds. Other compounds (AZD6244, U0126, and CI-1040) could only induce the appearance of 10%–15% MBP^+ cells at the most effective doses (Figure 3a,b). Treatment of OPCs with these compounds (at the most effective dose in inducing OPC to OL differentiation) for 15 min almost completely inhibited the phosphorylation of ERK1/2 (Figure 3c). Interestingly, when compound treatment lasted for 4 days (medium containing compounds was refreshed once at Day 3), only PD0325901 and AZD8330 showed complete inhibition of ERK1/2 phosphorylation, which correlated well with high levels of MBP detected in the same group (Figure 3d). These results indicate that inhibiting MAPK/ERK pathway promotes OL generation, and the duration of MAPK/ERK inhibition might be critical in enhancing the differentiation process.

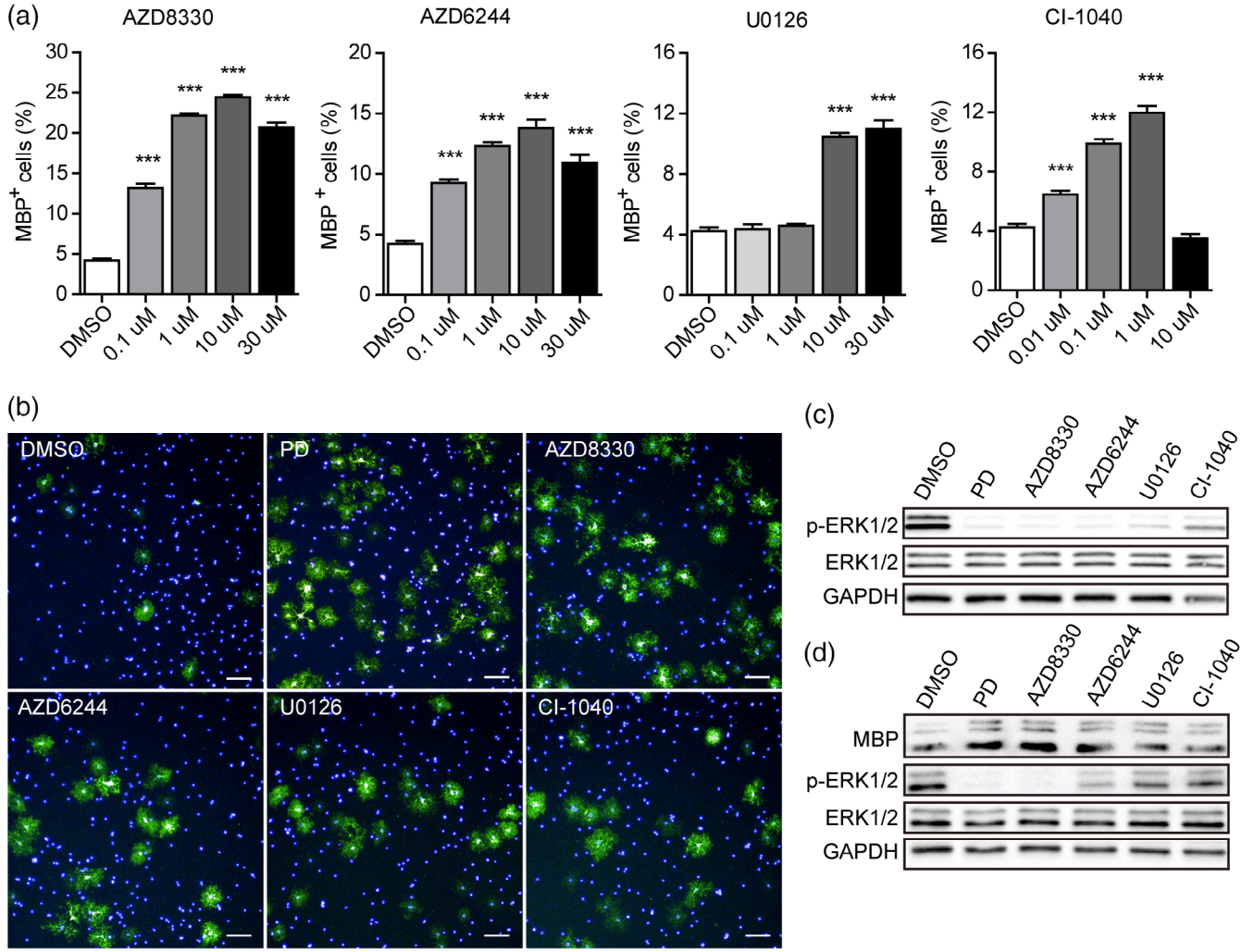

FIGURE 3 Inhibition of ERK/MAPK pathway promotes OL differentiation. (a) Dose-dependent effects of four MEK inhibitors, AZD8330, AZD6244, U0126, and CI-1040, in inducing OPC differentiation into mature OLs. Mouse NPC-derived OPCs were treated with various compounds for 4 days. Cells were stained with antibody against MBP (green). Nuclei were stained with Hoechst (blue). Data are representative of three independent experiments, means ± SEM (n = 4). ***p < .001 (one-way ANOVA followed by Dunnett's multiple comparison test). (b) Representative images of OLs induced by compounds at their most effective concentration (PD0325901, AZD8330, AZD6244, and U0126 at 10 μM; CI-1040 at 1 μM). Scale bars, 100 μm. (c,d) OPCs were treated with PD0325901 (10 μM), AZD8330 (10 μM), AZD6244 (10 μM), U0126 (10 μM), or CI-1040 (1 μM) for 15 min (c) or 4 days (d). Cells were harvested for western blot analysis [Color figure can be viewed at wileyonlinelibrary.com]

3.3 | PD0325901 enhances myelination in OPC–DRG neuron co-culture in vitro

PD0325901's effect in promoting OPC to OL differentiation was further studied in primary OPCs. PD0325901 was found to dose dependently increase the percentage of MBP^+-OLs generated from the primary OPCs (Figure 4a,b). Then we set up an in vitro myelination system by co-culturing primary OPCs with DRG neurons (O'Meara, Ryan, Holly, & Rashmi, 2011) to evaluate the effect of PD0325901 on myelin formation. Myelinated axons were quantified as co-localization of MBP^+ OL process and NFH^+ (also called NF-200, 200 kD neurofilament) axons (Huang et al., 2011). Compared to DMSO control, PD0325901 induced a concentration-dependent increase in the length of MBP^+NHF^+ myelinated axon in the co-culture (Figure 4c,d). These results indicate that decreased ERK/MAPK signaling not only promotes the generation of mature OLs from primary OPCs but also enhances myelin formation in vitro.

3.4 | PD0325901 promotes remyelination in EAE mice

MS and EAE are characterized by autoimmune-mediated demyelination and neurodegeneration. We next examined the effect of PD0325901 in the MOG-induced EAE model. PD0325901 (5 mg/kg) was administered prophylactically by a daily intraperitoneal (i.p.) injection from Day 3 post-immunization and was found to significantly reduce the disease scores compared to the vehicle control (Figure 5a). In parallel experiment, spinal cords from PD0325901- or vehicle-treated mice were isolated at Day 21 postimmunization. OLs and OPCs in the spinal cord lesions were assessed by immunostaining with antibodies that recognize markers of mature OLs (MBP and GST-pi) and OPCs (NG2) (Figure 5b-d). Severe demyelination occurred in the spinal cord of EAE mice as some areas in the white matter lost MBP staining (Figure 5b,e) and the number of $GST\text{-}pi^+$ cells was also reduced significantly (Figure 5c,f). And in the demyelinated spinal cord, a substantial number of $NG2^+$ OPCs were

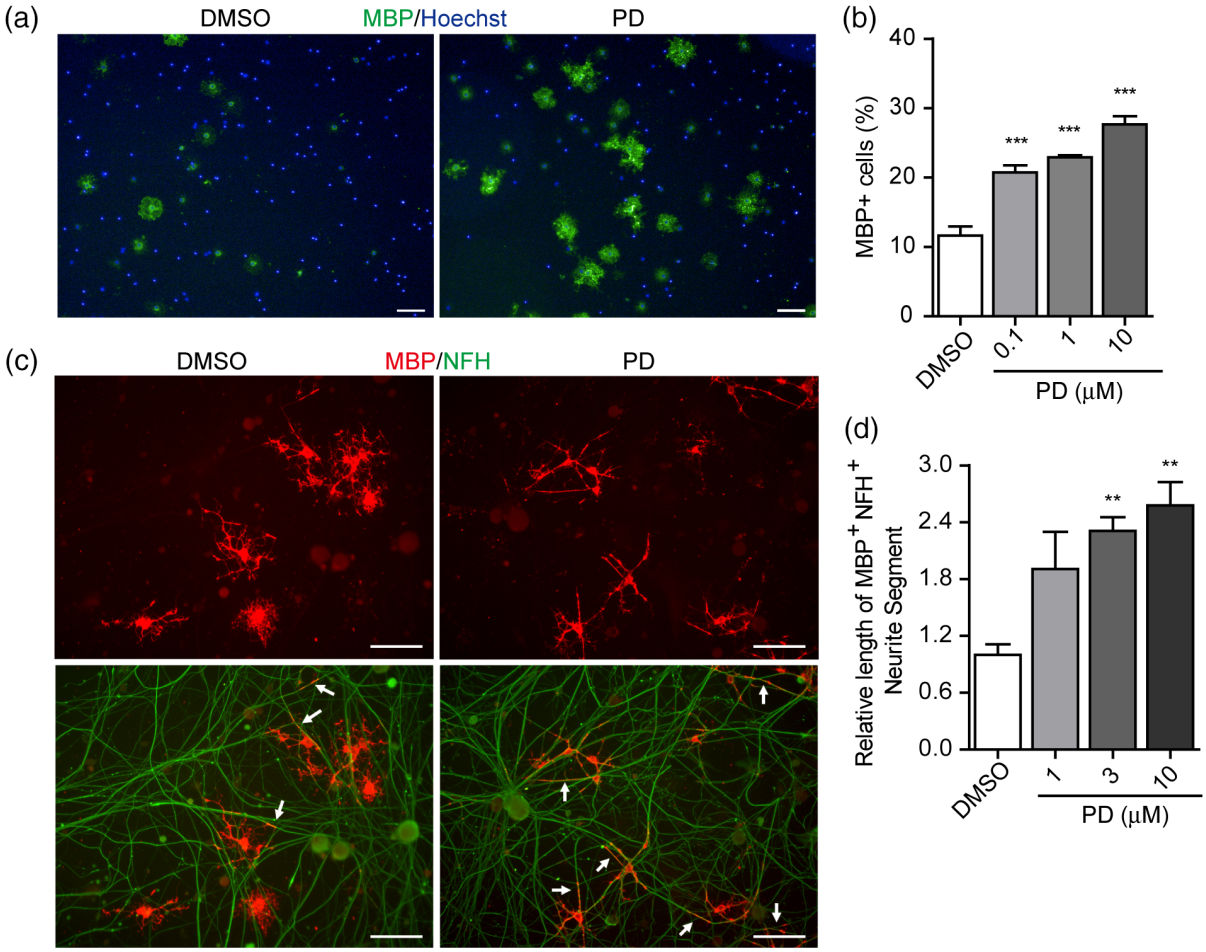

FIGURE 4 PD0325901 enhances myelination in vitro. (a,b) Effect of PD0325901 in inducing differentiation of mouse primary NG2$^+$ OPCs. Mouse primary NG2$^+$ OPCs were induced to differentiation in the presence of DMSO or PD0325901 for 4 days. Cells were stained for MBP (green) and nuclei (Hoechst, blue). Scale bars, 100 μm. Representative images (a, PD0325901 at 10 μM) and statistical analysis (b) of the MBP$^+$ cells. Data are representative of three independent experiments, means ± SEM (n = 3). ***p < .001 versus DMSO control (one-way ANOVA followed by Dunnett's multiple comparison test). (c,d) Effect of PD on myelin formation in vitro. Primary OPCs were co-cultured with DRG–neurons in the presence of vehicle or PD0325901 for 6 days. Cells were fixed and immunostained for NFH (neurofilament, green) and MBP (OLs, red). Arrows indicate myelinated axons (double positive for NFH and MBP). Scale bars, 100 μm. Representative images (c, PD0325901 at 10 μM) and statistical analysis (d) of myelinated axons in OPC–DRG neuron co-cultures. Data are representative of three independent experiments, means ± SEM (n = 4). **p < .01 versus DMSO control (one-way ANOVA followed by Dunnett's multiple comparison test) [Color figure can be viewed at wileyonlinelibrary.com]

observed in the white matter region (Figure 5d,g). In PD0325901-treated mice, demyelination was significantly mitigated with increased number of GST-pi$^+$ mature OLs, and reduced number of NG2$^+$ OPCs (Figure 5b–g). Furthermore, g-ratios (axonal diameter to total myelinated fiber diameter) of remyelinated spinal cord axons were analyzed by transmission electron microscopy. Demyelination was evidenced by increased g-ratio in EAE mice compared to naive ones (Figure 5h–j). PD0325901 treatment significantly reduced g-ratios in EAE mice, indicating a better recovery (Figure 5h–j). These observations suggest that inhibition of MAPK/ERK signaling may promote remyelination in EAE mice by enhancing OPC to OL differentiation.

However, whether PD0325901 affects the immune part of the EAE model remains elusive. The pathogenic cells in EAE are mainly CD4$^+$ T cells, especially the Th17 and Th1 subgroups. A previous study has reported that blockade of ERK attenuates EAE by inhibiting the induction of Th1 and Th17 cells (Brereton, Sutton, Lalor, Lavelle, & Mills, 2009). Other studies have demonstrated that blockade of ERK promotes Th17 differentiation (Cui et al., 2009; Tan & Lam, 2010) without affecting the Th1 subset (Cui et al., 2009). And inhibition of ERK does not significantly affect Th17 production has also been reported (Lu et al., 2010). The conclusion from previous studies has been controversial.

To further confirm the ability of PD0325901 in enhancing remyelination in vivo, we conducted the T-cell-independent cuprizone-induced demyelination model (Doan et al., 2013; Matsushima & Morell, 2001).

3.5 | PD0325901 promotes myelin recovery in drug-induced demyelination model

Mice were fed with a diet containing 0.2% (w/w) cuprizone for 5 weeks to induce complete demyelination (Figure 6a–c). Upon cuprizone withdrawal, vehicle or PD0325901 (10 mg/kg) was administrated by daily i.p. injection for 1 or 2 weeks (Figure 6a). Mice were euthanized and myelination at the corpus callosum was evaluated by Luxol fast blue

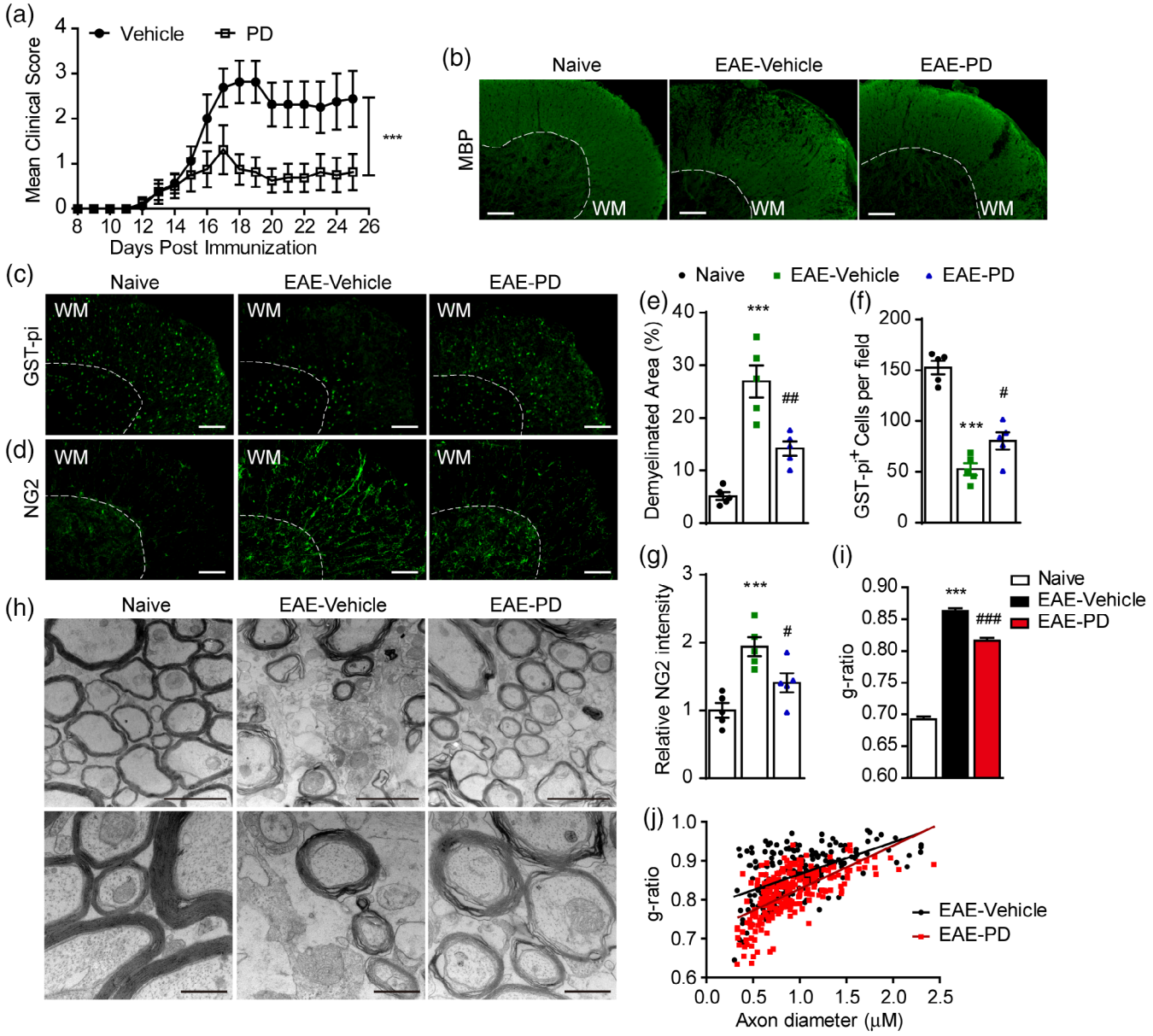

FIGURE 5 PD0325901 promotes remyelination in MOG-induced EAE model. (a) Clinical scores of C57BL/6 EAE mice treated with PD0325901 (5 mg/kg) or vehicle once daily via intraperitoneal injection from Day 3 postimmunization till the end of the study. Data are means ± SEM (n = 8). ***p < .001 (two-way ANOVA). (b–d) Representative images of immunostaining of OL markers (MBP and GSI-pi) and OPC marker (NG2) in the spinal cords isolated on Day 21 postimmunization from EAE mice treated with PD0325901 (5 mg/kg) or vehicle. Scale bars, 100 μm. (e–g) Quantification of demyelination area (MBP^- area in b) in white matter (e), GST-pi^+ cells (f), and NG2 intensity (g). Five animals from each group were sacrificed and four sections of the spinal cord of each animal were analyzed. Data are means ± SEM. ***p < .001 versus Naive group, $^{\#}p$ < .05, $^{\#\#}p$ < .01, versus vehicle group (one-way ANOVA followed by Tukey's multiple comparison test). (h) Representative electron microscopy images of spinal cords isolated on Day 21 postimmunization from EAE mice treated with PD0325901 (5 mg/kg) or vehicle. Scale bars, top panels, 2 μm; bottom panels, 0.5 μm. (i) g-ratios of spinal cord axons in (h). Data are means ± SEM. (n = 200), ***p < .001 versus Naive group, $^{\#\#\#}p$ < .001 versus vehicle group (one-way ANOVA followed by Tukey's multiple comparison test). (j) The scatter plot displaying the individual g-ratio values and axonal size distribution [Color figure can be viewed at wileyonlinelibrary.com]

staining (Berghoff et al., 2017; Deshmukh et al., 2013). Spontaneous remyelination could be observed in the vehicle-treated group, and PD0325901 treatment further accelerated the remyelination process (Figure 6b,c). The effect of PD0325901 was further assessed by immunofluorescent staining of myelin proteins MBP and MOG, and mature OL marker GST-pi in the corpus callosum region after 2-week treatment with PD0325901. Consistent with Luxol fast blue staining, PD0325901 treatment significantly increased the staining of MBP and MOG, and the number of GST-pi^+ OLs (Figure 6d–f). Moreover, less PDGFRα^+ OPCs were detected in PD0325901-treated group (Figure 6d,f), suggesting that PD0325901 promotes in vivo remyelination by enhancing OPC differentiation.

The myelin status was further evaluated by transmission electron microscopy. After 5 weeks of cuprizone treatment, very few axons in corpus callosum remained myelinated (Figure 6g–i). Two weeks after cuprizone withdrawn, spontaneous remyelination could

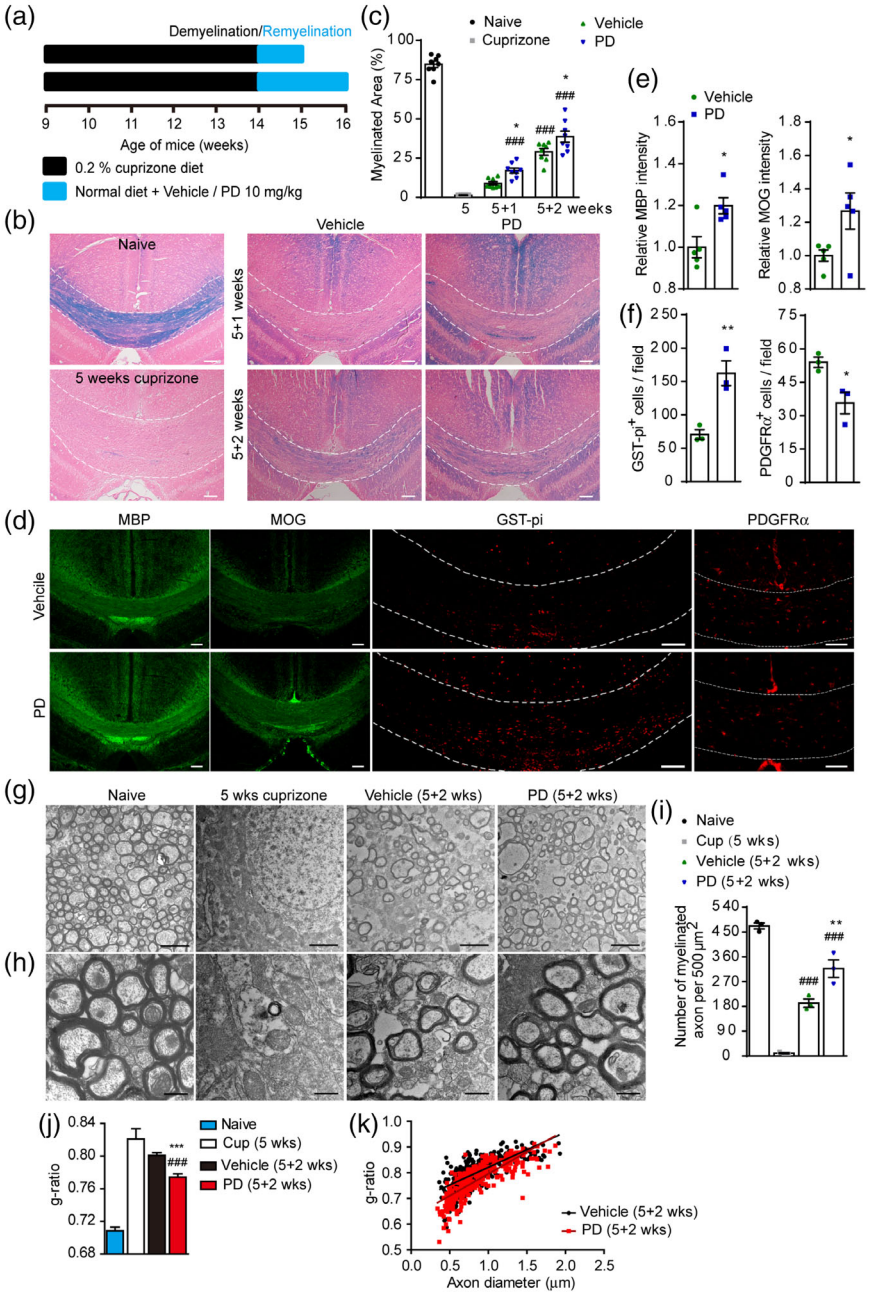

FIGURE 6 PD0325901 promotes remyelination in cuprizone-induced demyelination model. (a) A schematic drawing of the cuprizone induced demyelination/remyelination mice model. Demyelination was induced in C57BL/6 mice by feeding with a diet containing 0.2% cuprizone for 5 weeks. Following cuprizone withdrawal, mice were treated with vehicle or PD0325901 (10 mg/kg) for 1 or 2 weeks. (b) Representative images of the corpus callosum region stained with Luxol fast blue after cuprizone and PD0325901 treatment. Scale bars, 100 μm. (c) Quantification of the myelinated areas in (b). Data are means ± SEM. Eight mice per group, five sections of the corpus callosum region from each mouse were analyzed. $^{###}p < .001$ versus cuprizone group, $^{*}p < .05$, versus vehicle group (one-way ANOVA followed by Bonferroni's multiple comparison test). (d) Representative images of sections from the corpus callosum region of the brains isolated from PD0325901- or vehicle-treated mice (5 + 2 weeks) immunostained for MBP, MOG, GST-pi, and PDGFRα. Scale bars, 100 μm. (e) Quantification of the fluorescent intensity of MBP, MOG in corpus callosum as presented in (d). Data are means ± SEM (five mice per group, five sections from each mouse were analyzed). $^{*}p < .05$, versus vehicle group (Student's *t* test). (f) Quantification of the number of GST-pi^{+}, PDGFRα^{+} cells in corpus callosum as presented in (d). Data are means ± SEM (three mice per group; six sections from each mouse were analyzed). $^{*}p < .05$, $^{**}p < .01$ versus vehicle group (Student's *t* test). (g,h) Representative electron microscopy images of the corpus callosum region isolated from cuprizone-fed mice treated with PD0325901 (10 mg/kg) or vehicle for 2 weeks (5 + 2 weeks). Scale bars in (g), 2 μm. Scale bars in (h), 0.5 μm. (i) Quantification of the myelinated axons from (g). Data are means ± SEM (three mice per group, five sections from each mouse were analyzed). $^{###}p < .001$ versus cuprizone group, $^{**}p < .01$ versus vehicle group (one-way ANOVA followed by Tukey's multiple comparison test). (j) Quantification of the *g*-ratios of the remyelinated axons in (g). Data are means ± SEM (n = 300, ~100 myelinated axons counted per mouse, three mice per group. As demyelination was thorough, only 48 myelinated axons were counted in Cuprizone [5 weeks] group), $^{###}p < .001$ versus cuprizone group, $^{***}p < .001$ versus vehicle group (one-way ANOVA followed by Tukey's multiple comparison test). (k) The scatter plot displaying the individual *g*-ratio values and axonal size distribution [Color figure can be viewed at wileyonlinelibrary.com]

be observed as the number of myelinated axons was significantly increased (Figure 6g–i). The PD0325901-treated animals had more myelinated axons (Figure 6g–i) and lower g-ratio (Figure 6j,k), indicating an even better recovery than the control group.

4 | DISCUSSION

ERK is a key component of the RAS/RAF/MEK/ERK signaling pathway that regulates cell survival, cell cycle entry, proliferation, and differentiation. Here, we demonstrated that reduction of ERK1/2 activity in NPC-derived OPCs, as well as primary OPCs, is sufficient to promote OLs differentiation and myelin formation both in vitro and in vivo. Thus, our study reveals a negative role of ERK1/2 signaling in OPC differentiation and remyelination.

It has been suggested that increased levels of ERK1/2 activity have detrimental effects on Schwann cells in the peripheral nervous system. Schwann cells are regenerative. A myelinating Schwann cell can regain the potential to proliferate in response to nerve injury. The dedifferentiated Schwann cells then redifferentiate during the repair process. in vitro studies have shown that activation of ERK1/2 signaling prevents the proliferating Schwann cells to differentiate in response to cAMP, induces dedifferentiation and downregulation of myelin proteins in myelinating Schwann cells, and induces demyelination in Schwann cell-DRG co-cultures (Harrisingh et al., 2004; Ogata et al., 2004). Furthermore, sustained elevation of ERK1/2 activity in myelinating Schwann cells of the adult peripheral nerves leads to dedifferentiation and demyelination, and pharmacologically inhibition of ERK signaling delays such detrimental effects (Napoli et al., 2012).

However, the role of ERK1/2 signaling in OLs in the CNS is more complicated and conflict results have been reported. A number of studies demonstrated increased levels of ERK1/2 activity also have detrimental effects in OLs, similar to Schwann cells. High dose of glial growth factor, an isoform of neuregulin1, or basic fibroblast growth factor (bFGF), induces strong ERK1/2 activation in mature OLs in vitro, which is concomitant with phenotypic reversion of OLs, downregulation of myelin proteins and aberrant cell cycle re-entry (Bansal & Pfeiffer, 1997; Canoll, Kraemer, Teng, Marchionni, & Salzer, 1999; Fressinaud, Vallat, & Labourdette, 1995). Other studies have reported that pharmacological inhibition of ERK1/2 signaling negatively regulates transition of early progenitors to the late progenitor stage, but does not affect the maturation of OLs (Baron, Metz, Bansal, Hoekstra, & de Vries, 2000; Guardiola-Diaz, Ishii, & Bansal, 2012). One study has claimed that ERK1/2 signaling promotes OL myelination in vitro (Xiao et al., 2012). However, none of these studies has carefully evaluated the dose effect of MEK inhibitors on OPC to OL differentiation. Our study shows that inhibition of ERK1/2 signaling dramatically promotes OPC differentiation and OL maturation. One possible explanation for the difference between our study and those three studies might be the use of different stage of OPCs as starting cells. Those previous studies used either partial or totally $O4^+$ progenitors, or even later stage $GalC^+$ progenitors. In contrast, NPC-derived $NG2^+O4^-$ OPCs were used as starting cells in our study. It is possible that the OPCs at $NG2^+O4^-$ stage are more proliferative, when these cells exit cell cycle and undergo differentiation, the reduction of ERK1/2 signaling may promote this process.

Several in vivo studies have shown that genetic loss- or gain-of-function of ERK1/2 in OL-lineage cells or Schwann cells lead to dramatic changes in myelin sheath thickness (Ishii, Furusho, & Bansal, 2013; Ishii, Fyffe-Maricich, Furusho, Miller, & Bansal, 2012; Newbern et al., 2011). Conditional deletion of ERK2 in CNP^+ cells on an ERK1 null background leads to reduction of myelin sheath thickness without affecting OPC proliferation and differentiation, as mutants fail to upregulate the major myelin genes during active myelination (Ishii et al., 2012). Likewise, sustained activation of ERK1/2 via the expression of constitutive active MEK1 using the CNP-Cre driver significantly increases myelin sheath thickness during development, which is independent of OPC to OL differentiation or initiation of myelination (Ishii et al., 2013). In the same study, increased activity of ERK1/2 in $Olig1^+$ cells results in transient hyperproliferation and overproduction of OPCs, but the number of myelinating OLs remains unchanged, and loss of ERK1/2 function in $Olig1^+$ cells reduces OPC proliferation and number, but does not directly reduce their capacity to differentiate into OLs (Ishii et al., 2013).

Interestingly, deletion of ERK2 in $Olig2^+$ cells on an ERK1 null background leads to reduced proliferation of $PDGFR\alpha^+$ OPCs, and a more ramified, complex morphology of $S100\beta^+$ OLs, suggesting that loss of ERK1/2 triggers premature differentiation which is also evidenced by a clear increase in MBP labeling in vivo (Newbern et al., 2011). The early lethality of $Erk1/2^{CKO(Olig2)}$ mice limited the analysis to only the initial stages of myelination. But these results imply a negative role of ERK1/2 signaling on OL differentiation and myelination, conflicted with previous studies mentioned above and supported our findings.

Most of these genetic manipulations are not time-dependent, which may complicate things further. There is a study that evaluated the role of ERK1/2 signaling in remyelination using the mice expressing constitutively active MEK1 under the control of CNP-Cre driver (Fyffe-Maricich, Schott, Karl, Krasno, & Miller, 2013). In mutant mice, thicker myelin sheath in remyelinated axons was observed. But a question was also raised that the demylination extent may differ in WT and mutant mice as upregulated ERK1/2 signaling in mutant mice sustains a whole lifetime. Our study specifically modulated ERK1/2 signaling in the remyelination process by compound treatment without affecting the demyelination process, which clearly demonstrated that pharmacological inhibition of ERK1/2 signaling can enhance remyelination through promoting OL differentiation. A time-dependent gene manipulation strategy might provide detailed information about the role of ERK1/2 in OL differentiation and myelin development and repair.

Use of small-molecule inhibitors might provide more time-specific manipulation of the pathway. Our in vitro study demonstrated that inhibition of ERK1/2 signaling with chemicals promotes the progression of $NG2^+O4^-$ early progenitors to mature OLs. And either shortened treatment duration or delayed intervention time point attenuates differentiation efficiency, which may explain the different conclusions drawn from different studies. Our in vivo study specifically modulated ERK1/2 signaling in the remyelination process by compound treatment without affecting the demyelination process, which clearly demonstrated that pharmacological inhibition of ERK1/2 signaling enhances remyelination through promoting OPC to OL differentiation.

ACKNOWLEDGMENTS

This work was supported by grants from the Ministry of Science and Technology of China (2015CB964503, 2017YFA0104002), the Chinese Academy of Sciences (XDA16010202), and the National Natural Science Foundation of China (81425024, 81730099, and 81472862).

CONFLICT OF INTEREST

The authors declare no conflict of interest.

AUTHOR CONTRIBUTION

N.S. conducted most of the experiments, analyzed the results, and wrote the manuscript. Y.G. performed the co-culture experiment and part of the OPC differentiation assay. B.H. performed part of the western blot. H.G. provided technical assistance in compounds. X.X. conceived the idea for the project, analyzed the results, and wrote the manuscript. All authors reviewed the results and approved the manuscript.

ORCID

Xin Xie https://orcid.org/0000-0003-2314-4800

REFERENCES

Akinleye, A., Furqan, M., Mukhi, N., Ravella, P., & Liu, D. (2013). MEK and the inhibitors: From bench to bedside. *Journal of Hematology & Oncology*, *6*(1), 27.

Bansal, R., & Pfeiffer, S. E. (1997). FGF-2 converts mature oligodendrocytes to a novel phenotype. *Journal of Neuroscience Research*, *50*(2), 215–228.

Barateiro, A., & Fernandes, A. (2014). Temporal oligodendrocyte lineage progression: in vitro models of proliferation, differentiation and myelination. *Biochimica et Biophysica Acta*, *1843*(9), 1917–1929. https://doi.org/10.1016/j.bbamcr.2014.04.018

Baron, W., Metz, B., Bansal, R., Hoekstra, D., & de Vries, H. (2000). PDGF and FGF-2 signaling in oligodendrocyte progenitor cells: Regulation of proliferation and differentiation by multiple intracellular signaling pathways. *Molecular and Cellular Neuroscience*, *15*(3), 314–329. https://doi.org/10.1006/mcne.1999.0827

Berghoff, S. A., Gerndt, N., Winchenbach, J., Stumpf, S. K., Hosang, L., Odoardi, F., … Stassart, R. (2017). Dietary cholesterol promotes repair of demyelinated lesions in the adult brain. *Nature Communications*, *8*, 14241.

Bergles, D. E., & Richardson, W. D. (2015). Oligodendrocyte development and plasticity. *Cold Spring Harbor Perspectives in Biology*, *8*(2), a020453. https://doi.org/10.1101/cshperspect.a020453

Brereton, C. F., Sutton, C. E., Lalor, S. J., Lavelle, E. C., & Mills, K. H. (2009). Inhibition of ERK MAPK suppresses IL-23- and IL-1-driven IL-17 production and attenuates autoimmune disease. *Journal of Immunology*, *183*(3), 1715–1723. https://doi.org/10.4049/jimmunol.0803851

Canoll, P. D., Kraemer, R., Teng, K. K., Marchionni, M. A., & Salzer, J. L. (1999). GGF/neuregulin induces a phenotypic reversion of oligodendrocytes. *Molecular and Cellular Neuroscience*, *13*(2), 79–94. https://doi.org/10.1006/mcne.1998.0733

Chang, A., Nishiyama, A., Peterson, J., Prineas, J., & Trapp, B. D. (2000). NG2-positive oligodendrocyte progenitor cells in adult human brain and multiple sclerosis lesions. *Journal of Neuroscience*, *20*(17), 6404–6412.

Chen, Y., Balasubramaniyan, V., Peng, J., Hurlock, E. C., Tallquist, M., Li, J., & Lu, Q. R. (2007). Isolation and culture of rat and mouse oligodendrocyte precursor cells. *Nature Protocols*, *2*(5), 1044–1051. https://doi.org/10.1038/nprot.2007.149

Craig, A., Luo, N. L., Beardsley, D. J., Wingate-Pearse, N., Walker, D. W., Hohimer, A. R., & Back, S. A. (2003). Quantitative analysis of perinatal rodent oligodendrocyte lineage progression and its correlation with human. *Experimental Neurology*, *181*(2), 231–240. https://doi.org/10.1016/S0114-4886(03)00032-3

Cui, G., Qin, X., Zhang, Y., Gong, Z., Ge, B., & Zang, Y. Q. (2009). Berberine differentially modulates the activities of ERK, p38 MAPK, and JNK to suppress Th17 and Th1 T cell differentiation in type 1 diabetic mice. *The Journal of Biological Chemistry*, *284*(41), 28420–28429. https://doi.org/10.1074/jbc.M109.012674

Deshmukh, V. A., Tardif, V., Lyssiotis, C. A., Green, C. C., Kerman, B., Kim, H. J., … Lairson, L. L. (2013). A regenerative approach to the treatment of multiple sclerosis. *Nature*, *502*(7471), 327–332. https://doi.org/10.1038/nature12647

Doan, V., Kleindienst, A. M., McMahon, E. J., Long, B. R., Matsushima, G. K., & Taylor, L. C. (2013). Abbreviated exposure to cuprizone is sufficient to induce demyelination and oligodendrocyte loss. *Journal of Neuroscience Research*, *91*(3), 363–373. https://doi.org/10.1002/jnr.23174

Du, C., Duan, Y., Wei, W., Cai, Y., Chai, H., Lv, J., … Xie, X. (2016). Kappa opioid receptor activation alleviates experimental autoimmune encephalomyelitis and promotes oligodendrocyte-mediated remyelination. *Nature Communications*, *7*, 11120. https://doi.org/10.1038/ncomms11120

Emery, B. (2010). Regulation of Oligodendrocyte differentiation and myelination. *Science*, *330*(6005), 779–782. https://doi.org/10.1126/science.1190927

Franklin, R. J. (2002). Why does remyelination fail in multiple sclerosis? *Nature Reviews. Neuroscience*, *3*(9), 705–714. https://doi.org/10.1038/nrn917

Franklin, R. J., & Ffrench-Constant, C. (2008). Remyelination in the CNS: From biology to therapy. *Nature Reviews. Neuroscience*, *9*(11), 839–855. https://doi.org/10.1038/nrn2480

Fressinaud, C., Vallat, J. M., & Labourdette, G. (1995). Basic fibroblast growth-factor down-regulates myelin basic-protein gene-expression and alters myelin compaction of mature oligodendrocytes in-vitro. *Journal of Neuroscience Research*, *40*(3), 285–293. https://doi.org/10.1002/jnr.490400302

Funfschilling, U., Supplie, L. M., Mahad, D., Boretius, S., Saab, A. S., Edgar, J., … Nave, K. A. (2012). Glycolytic oligodendrocytes maintain myelin and long-term axonal integrity. *Nature*, *485*(7399), 517–521. https://doi.org/10.1038/nature11007

Fyffe-Maricich, S. L., Schott, A., Karl, M., Krasno, J., & Miller, R. H. (2013). Signaling through ERK1/2 controls myelin thickness during myelin repair in the adult central nervous system. *Journal of Neuroscience*, *33*(47), 18402–18408. https://doi.org/10.1523/Jneurosci.2381-13.2013

Gensert, J. M., & Goldman, J. E. (1997). Endogenous progenitors remyelinate demyelinated axons in the adult CNS. *Neuron*, *19*(1), 197–203. https://doi.org/10.1016/S0896-6273(00)80359-1

Goldman, S. A., & Kuypers, N. J. (2015). How to make an oligodendrocyte. *Development*, *142*(23), 3983–3995. https://doi.org/10.1242/dev.126409

Guardiola-Diaz, H. M., Ishii, A., & Bansal, R. (2012). Erk1/2 MAPK and mTOR signaling sequentially regulates progression through distinct stages of oligodendrocyte differentiation. *Glia*, *60*(3), 476–486. https://doi.org/10.1002/glia.22281

Guo, Y. E., Suo, N., Cui, X., Yuan, Q., & Xie, X. (2018). Vitamin C promotes oligodendrocytes generation and remyelination. *Glia*, *66*, 1302–1316. https://doi.org/10.1002/glia.23306

Harrisingh, M. C., Perez-Nadales, E., Parkinson, D. B., Malcolm, D. S., Mudge, A. W., & Lloyd, A. C. (2004). The Ras/Raf/ERK signalling pathway drives Schwann cell dedifferentiation. *EMBO Journal*, *23*(15), 3061–3071. https://doi.org/10.1038/sj.emboj.7600309

Huang, J. K., Jarjour, A. A., Nait Oumesmar, B., Kerninon, C., Williams, A., Krezel, W., … Franklin, R. J. M. (2011). Retinoid X receptor gamma signaling accelerates CNS remyelination. *Nature Neuroscience*, *14*(1), 45–U68. https://doi.org/10.1038/nn.2702

Ishii, A., Furusho, M., & Bansal, R. (2013). Sustained activation of ERK1/2 MAPK in oligodendrocytes and schwann cells enhances myelin growth and stimulates oligodendrocyte progenitor expansion. *Journal of Neuroscience*, *33*(1), 175–186. https://doi.org/10.1523/JNEUROSCI.4403-12.2013

Ishii, A., Fyffe-Maricich, S. L., Furusho, M., Miller, R. H., & Bansal, R. (2012). ERK1/ERK2 MAPK signaling is required to increase myelin thickness

independent of oligodendrocyte differentiation and initiation of myelination. *Journal of Neuroscience*, *32*(26), 8855–8864. https://doi.org/10.1523/JNEUROSCI.0137-12.2012

Keirstead, H. S., Levine, J. M., & Blakemore, W. F. (1998). Response of the oligodendrocyte progenitor cell population (defined by NG2 labelling) to demyelination of the adult spinal cord. *Glia*, *22*(2), 161–170. https://doi.org/10.1002/(Sici)1098-1136(199802)22:2<161::Aid-Glia7>3.3.Co;2-Z

Lappe-Siefke, C., Goebbels, S., Gravel, M., Nicksch, E., Lee, J., Braun, P. E., … Nave, K. A. (2003). Disruption of Cnp1 uncouples oligodendroglial functions in axonal support and myelination. *Nature Genetics*, *33*(3), 366–374. https://doi.org/10.1038/ng1095

Lopez-Juarez, A., Titus, H. E., Silbak, S. H., Pressler, J. W., Rizvi, T. A., Bogard, M., … Ratner, N. (2017). Oligodendrocyte Nf1 controls aberrant notch activation and regulates myelin structure and behavior. *Cell Reports*, *19*(3), 545–557. https://doi.org/10.1016/j.celrep.2017.03.073

Lu, L., Wang, J., Zhang, F., Chai, Y., Brand, D., Wang, X., … Zheng, S. G. (2010). Role of SMAD and non-SMAD signals in the development of Th17 and regulatory T cells. *Journal of Immunology*, *184*(8), 4295–4306. https://doi.org/10.4049/jimmunol.0903418

Matsushima, G. K., & Morell, P. (2001). The neurotoxicant, cuprizone, as a model to study demyelination and remyelination in the central nervous system. *Brain Pathology*, *11*(1), 107–116.

Mei, F., Mayoral, S. R., Nobuta, H., Wang, F., Desponts, C., Lorrain, D. S., … Chan, J. R. (2016). Identification of the kappa-opioid receptor as a therapeutic target for oligodendrocyte remyelination. *Journal of Neuroscience*, *36*(30), 7925–7935. https://doi.org/10.1523/JNEUROSCI.1493-16.2016

Morrison, B. M., Lee, Y., & Rothstein, J. D. (2013). Oligodendroglia: Metabolic supporters of axons. *Trends in Cell Biology*, *23*(12), 644–651. https://doi.org/10.1016/j.tcb.2013.07.007

Najm, F. J., Madhavan, M., Zaremba, A., Shick, E., Karl, R. T., Factor, D. C., … Tesar, P. J. (2015). Drug-based modulation of endogenous stem cells promotes functional remyelination in vivo. *Nature*, *522*(7555), 216–220. https://doi.org/10.1038/nature14335

Napoli, I., Noon, L. A., Ribeiro, S., Kerai, A. P., Parrinello, S., Rosenberg, L. H., … Lloyd, A. C. (2012). A central role for the ERK-signaling pathway in controlling Schwann cell plasticity and peripheral nerve regeneration in vivo. *Neuron*, *73*(4), 729–742. https://doi.org/10.1016/j.neuron.2011.11.031

Nave, K. A., & Werner, H. B. (2014). Myelination of the nervous system: Mechanisms and functions. *Annual Review of Cell and Developmental Biology*, *30*, 503–533. https://doi.org/10.1146/annurev-cellbio-100913-013101

Newbern, J. M., Li, X., Shoemaker, S. E., Zhou, J., Zhong, J., Wu, Y., … Snider, W. D. (2011). Specific functions for ERK/MAPK signaling during PNS development. *Neuron*, *69*(1), 91–105. https://doi.org/10.1016/j.neuron.2010.12.003

O'Meara, R. W., Ryan, S. D., Holly, C., & Rashmi, K. (2011). Derivation of enriched oligodendrocyte cultures and oligodendrocyte/neuron myelinating co-cultures from post-natal murine tissues. *Journal of Visualized Experiments*, *54*(54), e3324–e3324.

Ogata, T., Iijima, S., Hoshikawa, S., Miura, T., Yamamoto, S., Oda, H., … Tanaka, S. (2004). Opposing extracellular signal-regulated kinase and Akt pathways control Schwann cell myelination. *Journal of Neuroscience*, *24*(30), 6724–6732. https://doi.org/10.1523/Jneurosci.5520-03.2004

Planz, O. (2013). Development of cellular signaling pathway inhibitors as new antivirals against influenza. *Antiviral Research*, *98*(3), 457–468. https://doi.org/10.1016/j.antiviral.2013.04.008

Saab, A. S., Tzvetanova, I. D., & Nave, K. A. (2013). The role of myelin and oligodendrocytes in axonal energy metabolism. *Current Opinion in Neurobiology*, *23*(6), 1065–1072. https://doi.org/10.1016/j.conb.2013.09.008

Scolding, N. J., Frith, S., Linington, C., Morgan, B. P., Campbell, A. K., & Compston, D. A. S. (1989). Myelin-oligodendrocyte glycoprotein (MOG) is a surface marker of oligodendrocyte maturation. *Journal of Neuroimmunology*, *22*(3), 169–176. https://doi.org/10.1016/0165-5728(89)90014-3

Sebolt-Leopold, J. S., Merriman, R., Omer, C., Tecle, H., Bridges, A., Klohs, W., … Leopold, W. R. (2004). The biological profile of PD 0325901: A second generation analog of CI-1040 with improved pharmaceutical potential. *Cancer Research*, *64*(7 Supplement), 925–925.

Takebayashi, H., & Ikenaka, K. (2015). Oligodendrocyte generation during mouse development. *Glia*, *63*(8), 1350–1356. https://doi.org/10.1002/glia.22863

Tan, A. H., & Lam, K. P. (2010). Pharmacologic inhibition of MEK-ERK signaling enhances Th17 differentiation. *Journal of Immunology*, *184*(4), 1849–1857. https://doi.org/10.4049/jimmunol.0901509

van Tilborg, E., de Theije, C. G. M., van Hal, M., Wagenaar, N., de Vries, L. S., Benders, M. J., … Nijboer, C. H. (2018). Origin and dynamics of oligodendrocytes in the developing brain: Implications for perinatal white matter injury. *Glia*, *66*(2), 221–238. https://doi.org/10.1002/glia.23256

Woodruff, R. H., Fruttiger, M., Richardson, W. D., & Franklin, R. J. M. (2004). Platelet-derived growth factor regulates oligodendrocyte progenitor numbers in adult CNS and their response following CNS demyelination. *Molecular and Cellular Neuroscience*, *25*(2), 252–262. https://doi.org/10.1016/j.mcn.2003.10.014

Xiao, J., Ferner, A. H., Wong, A. W., Denham, M., Kilpatrick, T. J., & Murray, S. S. (2012). Extracellular signal-regulated kinase 1/2 signaling promotes oligodendrocyte myelination in vitro. *Journal of Neurochemistry*, *122*(6), 1167–1180. https://doi.org/10.1111/j.1471-4159.2012.07871.x

Zhang, S. C. (2001). Defining glial cells during CNS development. *Nature Reviews. Neuroscience*, *2*(11), 840–843. https://doi.org/10.1038/35097593

How to cite this article: Suo N, Guo Y, He B, Gu H, Xie X. Inhibition of MAPK/ERK pathway promotes oligodendrocytes generation and recovery of demyelinating diseases. *Glia*. 2019; 67:1320–1332. https://doi.org/10.1002/glia.23606